

Design, Synthesis and Biological Evaluation of Novel *N*-Alkyl- and *N*-Acyl-(7-substituted-2-phenylimidazo[1,2-*a*][1,3,5]triazin-4-yl)amines (ITAs) as Novel A₁ Adenosine Receptor Antagonists

Ettore Novellino,* Enrico Abignente, Barbara Cosimelli, Giovanni Greco, Manuela Iadanza, Sonia Laneri, Antonio Lavecchia, and Maria Grazia Rimoli

Dipartimento di Chimica Farmaceutica e Tossicologica, Università di Napoli "Federico II",
Via D. Montesano, 49, 80131 Napoli, Italy

Federico Da Settimo and Giampaolo Primofiore

Dipartimento di Scienze Farmaceutiche, Università di Pisa, Via Bonanno 6, 56126 Pisa, Italy

Daniela Tuscano, Letizia Trincavelli, and Claudia Martini

Dipartimento di Psichiatria, Neurobiologia, Farmacologia e Biotecnologie, Università di Pisa,
Via Bonanno 6, 56126 Pisa, Italy

Received April 17, 2002

Prompted by pharmacophore and docking based models, we have synthesized and tested a number of *N*-alkyl and *N*-acyl-(7-substituted-2-phenylimidazo[1,2-*a*][1,3,5]triazin-4-yl)amines (ITAs, **7**) designed as a new class of A₁ adenosine receptor (A₁AR) antagonists. Binding affinities at the A₁AR, A_{2A}AR, and A₃AR were determined using bovine cerebral membranes. Most of the compounds displayed *K_i* values at the A₁AR in the submicromolar or even in the low nanomolar range, thus confirming the rationale leading to their synthesis. All or most of the ligands turned out to be selective for the A₁AR over the A_{2A}AR and A₃AR subtypes, respectively. Structure-affinity relationships at the A₁AR were rationalized by docking simulations in terms of putative ligand/receptor interactions. Among the ITAs investigated, 1-[(7-methyl-2-phenylimidazo[1,2-*a*][1,3,5]triazin-4-yl)amino]acetone (**7j**) exhibited the best combination of affinity at the A₁AR (*K_i* = 12 nM) and selectivity over the A_{2A}AR and A₃AR subtypes (*K_is* > 10000 nM).

Introduction

The activation of cell surface adenosine receptors (ARs) is predominantly responsible for the wide variety of effects produced by adenosine throughout several organ systems. The combination of pharmacological studies and molecular cloning have led to the discovery of the existence of at least four distinct adenosine receptors which have been identified and classified as A₁, A_{2A}, A_{2B}, and A₃. The responses of these four ARs are mediated by receptor-coupled G-proteins which activate several effector systems including adenylate cyclase, potassium and calcium channels, phospholipase A₂ or C, and guanylate cyclase.^{1–3}

On the basis of the widespread effects attributed to the accumulation of endogenously released adenosine, it has long been considered that regulation of ARs has substantial therapeutic potential.

The A₁ adenosine receptor (A₁AR) is the best known and the most comprehensively studied AR subtype, and during the last 20 years a large number of A₁AR agonists⁴ and antagonists^{5–7} have been developed. With regards to possible therapeutic application of A₁AR antagonist, effects on the cardiovascular system, kidney,

and CNS have been studied. Currently, A₁AR selective antagonists are developed as potassium-saving diuretics with kidney-protective properties, as general cognition enhancers for geriatric therapy, and for the treatment of acute renal failure and of CNS disorders such as Alzheimer disease.^{5–7}

We have recently described 3-aryl[1,2,4]triazino[4,3-*a*]benzimidazol-4(10*H*)-one (ATBI) derivatives as a new class of selective A₁AR antagonists.⁸ The most potent ATBI, compound **1**, displayed a *K_i* value of 18 nM on bovine cortical preparations. Pharmacophore- and docking-based modeling of **1** and other well-known A₁AR antagonists (**2–6**) (see Chart 1) suggested that these ligands could interact with three H-bond sites (HB1, HB2, and HB3) and three lipophilic pockets (L1, L2, and L3) within the receptor binding site. The Asn254 (helix VI) side chain CO and NH₂ moieties (HB1 and HB2, respectively) and the Ser277 (helix VII) hydroxyl (HB3 as a H-bond donor) group correspond to the H-bond centers. The above interactions are highlighted in Figure 1.

In pursuing our researches in this field we have investigated *N*-alkyl and *N*-acyl 7-substituted-2-phenylimidazo[1,2-*a*][1,3,5]triazin-4-ylamines (ITAs, **7a–r**), which fulfill the pharmacophore requirements for A₁AR antagonism (Figure 2). These compounds were prepared

* To whom all correspondence should be addressed. Tel: +39 081678643. Fax: +39 081678644. E-mail: novellino@unina.it.

Chart 1

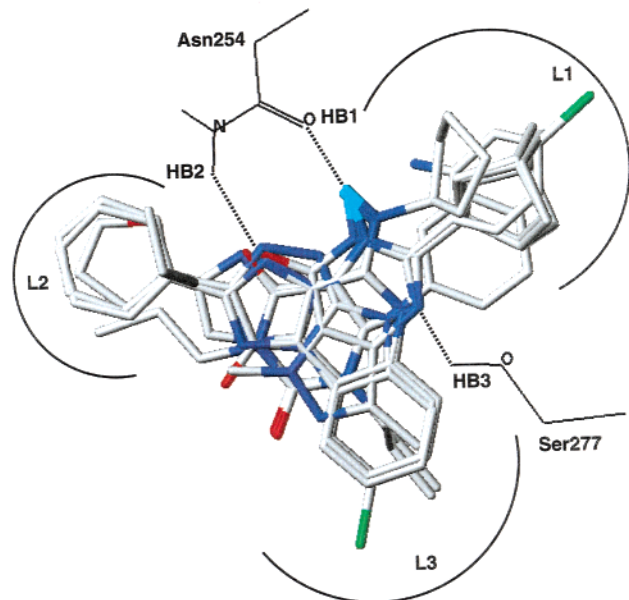
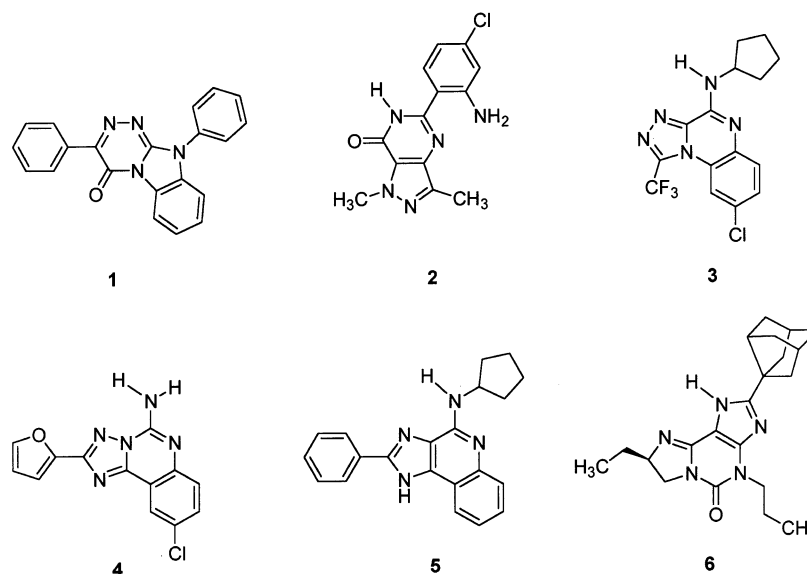


Figure 1. Pharmacophoric overlay of compounds **1-6**. HB1, HB2 and HB3 are H-bond sites of A₁AR corresponding to Asn254 (helix VI) and Ser277 (helix VII) side chains. L1, L2 and L3 map hydrophobic interactions. **1-6** are described in the following references: **1**,⁸ **2**,⁹ **3**,¹⁰ **4**,¹¹ **5**,¹² **6**.¹³

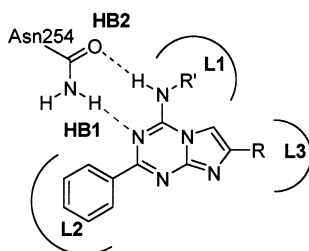


Figure 2. Pharmacophoric scheme of ITAs/A₁AR interaction.

following a versatile procedure similar to that described by us for isosteric imidazo[1,2-*a*]pyrimidines showing antiinflammatory activity.¹⁴

Selection of substituents R' and R at the N-4 and 7-position of the imidazotriazine nucleus was guided by

the results of docking simulations into our model of bovine A₁AR (details are given in the Experimental Section). Inspection of the L1 lipophilic pocket suggested that R' has to be hydrophobic and not exceedingly large. However, a less lipophilic R', such as CH₂COCH₃ would enable the carbonyl oxygen to accept one or two H-bonds from Ser277 and Thr91 (helix III) hydroxyls. Figure 3 shows the docking model of **7j** (R' = CH₂COCH₃, R = CH₃) featuring the two putative H-bonds described above.

A phenyl ring in position 2, supposed to fill the L2 site (Figure 2), was maintained fixed all through the ITA series. This substituent gave, in fact, the most potent ATBI (compound **1**) by interacting with the L2 lipophilic pocket.

Lead optimization efforts focused initially on the nature of R' by keeping fixed R = CH₃. Replacements of the 7-CH₃ with a 7-C₂H₅, a 7-*iso*C₃H₇, or a 7-Ph, to optimize the hydrophobic and steric interactions between R and the L3 site, were accomplished on a few selected structures.

The present paper describes the design, the synthesis, the biological evaluation, and the structure–activity relationships (SARs) of compounds with a general formula **7**.

Chemistry

The imidazo[1,2-*a*][1,3,5]triazine derivatives **7a-r** were prepared in two steps. First, the imidazo[1,2-*a*][1,3,5]triazines were synthesized using a synthetic method in which the starting 2,4-diamino-6-phenyl-[1,3,5]triazine **8** was warmed in refluxing ethanol with 2-chloroacetone **9**, 1-chlorobutan-2-one **10**, 1-bromo-3-methylbutan-2-one **11**, or 2-bromoacetophenone **12**, to obtain the corresponding 7-methyl-2-phenylimidazo[1,2-*a*][1,3,5]triazin-4-ylamine **7a**, 7-ethyl-2-phenylimidazo[1,2-*a*][1,3,5]triazin-4-ylamine **7b**, 7-isopropyl-2-phenylimidazo[1,2-*a*][1,3,5]triazin-4-ylamine **7c**, and 2,7-diphenylimidazo[1,2-*a*][1,3,5]triazin-4-ylamine **7d**, respectively (Scheme 1).

The correct structural assignments for these products were performed with ¹H and ¹³C NMR spectroscopy. In

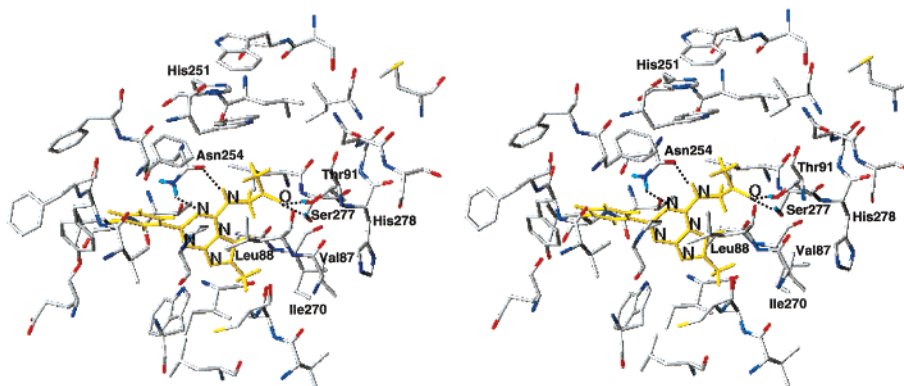
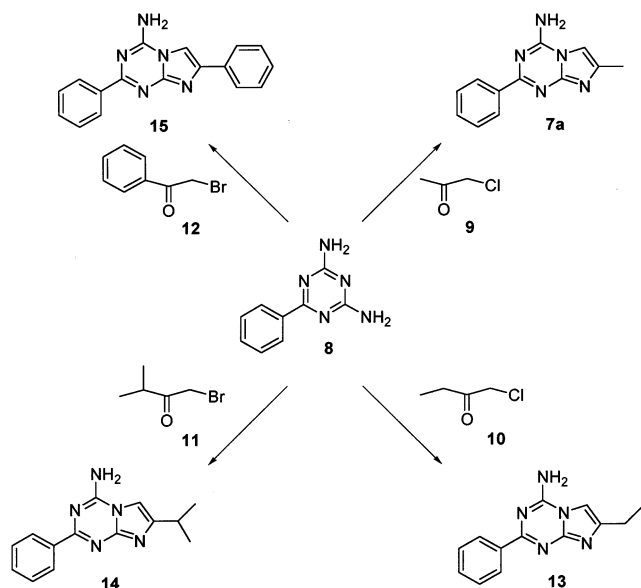


Figure 3. Model of the A₁AR binding site complexed with compound **7j**. Only amino acids located within 5 Å from any atom of the bound ligand are displayed. Dotted lines highlight ligand/receptor H-bonds.

Scheme 1



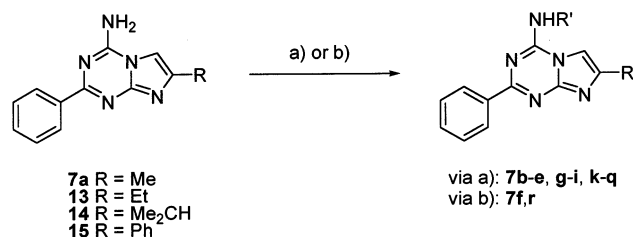
particular, the starting compound **8** is differently substituted in the 4 and 6 positions, so it was possible, in theory, to obtain a pair of isomeric products from the cyclocondensation reaction of this amine with the α -halo ketone derivatives **9**, **10**, **11**, and **12**. The correct structural assignment for products **7a**, **13**, **14**, and **15**, was obtained by a HMBC experiment. The carbon atom in the triazine ring that showed a correlation pathway with the phenyl hydrogen atoms (δ 162.9) was not correlated to the hydrogen atom into the imidazole ring (H-6, δ 7.35). This hydrogen, however, showed a correlation with the two carbon atoms (δ 152.4 and 152.3) in the triazine ring.

The amino group of compounds **7a**, **13**, **14**, and **15** was subsequently allowed to react with haloalkyl or acyl derivatives according to the condition described in the Experimental Section, and summarized in Scheme 2, to give the derivatives **7b–i, k–r**. The compound **7j** was obtained together **7a** by reaction of triazine **8** with 2-chloroacetone. The presence of carbonyl function in compounds **7j**, **7k**, **7o**, **7p**, and **7q** has been unequivocally ascertained on the basis of the IR spectra.

Results and Discussion

The binding affinity of each ITA derivative at the A₁ and A_{2A}ARs were determined in competition assays

Scheme 2^a

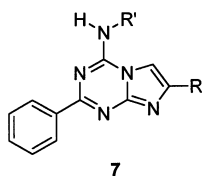


^a (a) R'Cl or R'Br, CH₃CN, K₂CO₃, KI; (b) (MeCO)₂O, 4-DMAP, THF.

of [³H]-N⁶-cyclohexyladenosine ([³H]CHA) and [³H]-2-[4-(2-carboxyethyl)phenethyl]amino-5'-(N-ethylcarbamoyl)adenosine ([³H]CGS 21680) to bovine cortical (A₁) and striatal (A_{2A}) membranes, respectively. Affinity at the A₃AR was determined in competition assays of [¹²⁵I]-N⁶-(3-iodo-4-aminobenzyl)-5'-N-methylcarboxamidoadenosine ([¹²⁵I]AB-MECA) to bovine cortical membranes in the presence of the A₁AR selective antagonist DPCPX (20 nM).⁸

The results of the binding experiments are summarized in Table 1. Most of the compounds display *K_i* values at the A₁AR in the sub-micromolar or even in the low nanomolar range, thus confirming the rationale leading to their synthesis. Most of the ligands turned out selective for the A₁AR over the A_{2A}AR and A₃AR subtypes. Those binding to the A₁AR with a high potency and selectivity are **7g**, **7j**, and **7n**. Moreover, compounds **7g**, **7l**, and **7m** are characterized by *K_i* values which represent a 3–5.5-fold gain in affinity with respect to that of the previously described most active ATBI derivative **1** (*K_i* 18 nM).

As stated in the Introduction, our research started with the 7-methyl derivatives **7a–k** seeking the optimal R' substituent. In the 7-methyl series **7a–k**, the parent compound **7a** showed a fair affinity at the A₁AR with a low selectivity toward A_{2A} (2-fold) and A₃ (6-fold) ARs. The affinity, as expected, is improved by a hydrophobic character of R' (hypothesized to fill the L1 lipophilic pocket as schematized in Figure 2). Indeed, introduction of an alkyl (cyclopentyl) substituent at N-4 (**7b**) determined an 8-fold enhancement in A₁AR potency and a parallel gain in selectivity vs A_{2A} and A₃ARs (100-fold and 55-fold, respectively). Bulkier alkyl and arylalkyl substituents at this position (**7c–e**) dramatically decreased A₁ and A_{2A}ARs affinity, while varying results were obtained at the A₃AR with respect to **7a**: an

Table 1. Binding Affinity Data of ITA Derivatives 7

no.	R	R'	K _i (nM) ^a		
			bA ₁ ^b	bA _{2A} ^c	bA ₃ ^d
7a	CH ₃	H	332 ± 130	682 ± 129	2000 ± 700
7b	CH ₃	cyclopentyl	41.0 ± 9.0	4100 ± 400	2250 ± 300
7c	CH ₃	1-adamantyl	511 ± 9.0	>10000	526 ± 13
7d	CH ₃	CH ₂ -cyclohexyl	231 ± 99	>10000	2100 ± 400
7e	CH ₃	CH ₂ Ph	3900 ± 1100	>10000	>10000
7f	CH ₃	COCH ₃	855 ± 60	>10000	231 ± 60
7g	CH ₃	CO-cyclopentyl	4.4 ± 1.2	4300 ± 300	410 ± 60
7h	CH ₃	CO-cyclohexyl	116 ± 75	>10000	202 ± 22
7i	CH ₃	COPh	27.2 ± 5.2	>10000	11.8 ± 1.1
7j	CH ₃	CH ₂ COCH ₃	12.0 ± 3.0	>10000	>10000
7k	CH ₃	CH ₂ COC ₂ H ₅	>10000	>10000	>10000
7l	C ₂ H ₅	CO-cyclopentyl	3.3 ± 1.1	2600 ± 200	20.2 ± 7.0
7m	<i>i</i> C ₃ H ₇	CO-cyclopentyl	5.8 ± 3.1	>10000	17.4 ± 10
7n	Ph	CO-cyclopentyl	17.0 ± 13.0	2500 ± 200	1240 ± 180
7o	C ₂ H ₅	CH ₂ COCH ₃	>10000	>10000	>10000
7p	<i>i</i> C ₃ H ₇	CH ₂ COCH ₃	2360 ± 800	>10000	3050 ± 800
7q	Ph	CH ₂ COCH ₃	>10000	>10000	5800 ± 900
7r	Ph	COCH ₃	23.0 ± 2.0	3200 ± 220	40.0 ± 3.3
DPCPX			0.5 ± 0.03	337 ± 28	>10000
NECA			14 ± 4	16 ± 3	73 ± 5
CI-IBMECA			890 ± 61	401 ± 25	0.22 ± 0.02

^a The K_i values are means ± SEM derived by an iterative curve-fitting procedure (program Prism, GraphPad, San Diego, CA).

^b Displacement of specific [³H]CHA binding in bovine cortical membranes. ^c Displacement of specific [³H] CGS21680 binding in bovine striatal membranes. ^d Displacement of specific [¹²⁵I]AB-MECA binding in bovine cortical membranes in the presence of 20 nM DPCPX or percentage of inhibition of specific binding at 1 μM concentration.

enhancement in affinity for **7c**, equipotency for **7d**, and a complete loss of affinity in the case of **7e**.

Also the introduction of an acetyl moiety at the N-4 (**7f**) reduced A₁ and A_{2A}AR affinity, while a 8.5-fold gain in potency was observed for the A₃AR. Notwithstanding, **7g** (R' = CO-cyclopentyl), **7h** (R' = CO-cyclohexyl), and **7i** (R' = COPh) showed an enhancement in A₁AR affinity vs **7a** by 75.5-fold, 3-fold and 12-fold, respectively, with a good selectivity toward A_{2A}AR but not A₃AR. Moreover, a comparison between **7h** (R' = CO-cyclohexyl) and the 2-fold less potent **7d** (R' = CH₂-cyclohexyl) suggests that the amidic CO in R' is indeed beneficial, provided that a sufficiently hydrophobic moiety occupies the L1 pocket. The favorable effect of the CO linker with respect to CH₂ might be ascribed to either an improved H-bond donor ability of the NH group and/or to a more precise orientation of R' into L1.

However, prompted by docking simulations, we also prepared **7j** featuring R' = CH₂COCH₃. This substituent is rather hydrophilic but nevertheless makes two H-bonds with the Ser277 and Thr91 side chains (see Figure 3). The significant gain in A₁AR potency (71-fold) and selectivity achieved by inserting a methylene spacer between the acetyl group and the N-4 (compare **7j** vs **7f**) confirmed our prevision. Finally, we observed a complete loss of affinity at all the three ARs when the acetyl moiety of **7j** was substituted with a propionyl one in **7k**.

In the 7-CH₃ series of ITAs, **7g** (R' = CO-cyclopentyl, K_i = 4 nM) achieves the highest potency. Replacement of the cyclopentyl of **7g** with a cyclohexyl to yield **7h** produces a 25-fold drop of affinity probably because the

latter ring is exceedingly large. Unfavorable steric effects of R' can be likewise observed on comparing **7b** vs **7c**, **7d** vs **7e** and **7j** vs **7k**. Regarding **7d** and **7e**, the steric differences between the CH₂-cyclohexyl and CH₂-phenyl groups seem to us essentially related to the different valence geometry about the endocyclic C1 atom (sp³ or sp² hybridized, respectively).

The two most potent 7-CH₃ derivatives, **7g** and **7j**, were then selected as leads for structural modifications aimed at optimizing the nature of the substituent R hypothesized to dock into the L3 lipophilic site (Figure 2). Accordingly, the 7-CH₃ in **7g** and **7j** was replaced with a 7-C₂H₅, a 7-*iso*C₃H₇ or a 7-Ph by synthesizing compounds **7l–n** and, respectively, **7o–q**.

In the CO-cyclopentyl series (**7l–n**) potency remained almost similar (**7l** K_i = 3.3 nM) to that of the parent compound **7g** (K_i = 4.4 nM), while selectivity, especially toward A₃AR, was lost. The CH₂COCH₃ series (**7o–q**) gave even worst results, both in affinity and selectivity.

The above results suggest that the A₁AR L3 cavity is filled with optimal shape complementarity by the C₂H₅ or CH₃ of **7l** and **7j**, respectively, so that bulkier substituents R cannot fit properly in this cavity. It is interesting to note that in the **7g**, **7l–n** and **7j**, **7o–q** series the R groups larger than the optimal ones reduce affinity to quite different extents (up to 4-fold or more than 200-fold, respectively). The moderate or dramatic impact of nonoptimal R substituents on affinity strictly depends on the nature of R'. In other words, the effects of R and R' are not additive but interdependent.

In light of the docking model of **7j** (Figure 3), we speculate that the strong H-bonds accepted by the

carbonyl oxygen of CH₂COCH₃ from Ser277 and Thr91 hydroxyls somehow “freeze” the mobility of the complexed ligand. This implies that the steric hindrance arising from insertion of a relatively large substituent R cannot be counterbalanced through rotations and translations of the ligand to adapt R into the L3 pocket. Alternatively, accommodation of R into the L3 cavity would disrupt the putative H-bonds described above. If R' is not engaged in H-bonds with L1 (i.e., CO-cyclopentyl), the ligand can more freely move within the binding site, thus minimizing the steric repulsion between R and the L3 pocket.

To test our “dynamic” model of ITA/A₁AR interaction, we synthesized and assayed **7r** which combines a substituent R' smaller than CO-cyclopentyl (COCH₃) with a large R (Ph). In this case the replacement of the 7-CH₃ with a 7-Ph leads to a 37-fold improvement of affinity (compare **7r** vs **7f**) reaching a K_i value of 23 nM. The remarkable beneficial effect of 7-Ph in **7r** might be related to an “easier” positioning of the small COCH₃ into the L1 cavity, which in turn facilitates the anchoring of 7-Ph into the L3 site. Unfortunately, this enhancement in the affinity for A₁AR was paralleled by A₃AR potency (K_i = 40 nM), with a consequent decrease in A₁/A₃ selectivity.

Conclusions

Prompted by pharmacophore- and docking-based models, we have synthesized and tested a series of *N*-alkyl and *N*-acyl-(7-substituted-2-phenylimidazo[1,2-*a*][1,3,5]-triazin-4-yl)amines (ITAs, **7**) designed as a new class of A₁AR antagonists. Nonadditive, but interdependent, effects of R and R' substituents on A₁AR affinity could be rationalized by our docking model. The most interesting compound within this series is **7j** (R' = CH₂COCH₃ and R = CH₃) which exhibits the best combination of affinity at the A₁AR (K_i = 12 nM) and selectivity over the A_{2A}AR and A₃AR subtypes (K_is > 10000 nM).

Experimental Section

Chemistry. The course of reactions and purity of products were controlled by TLC, using precoated silica gel plates (Merck 60 F254) and chloroform/methanol 95:5 as eluant. Preparative separation was performed in columns containing Merck 60 silica gel (70–230 mesh ASTM) and with a Flash 40i chromatography module using preppacked cartridge system (Biotage). Melting points were determined with a Kofler hot stage microscope and are uncorrected.

Elemental analysis was within ±0.4% of the theoretical values. ¹H, ¹³C NMR, and HMBC experiments were recorded using a Bruker WM-250 or AMX-500 spectrometer, equipped with a Bruker X-32 computer. Chemical shift values are reported in δ units (ppm) relative to TMS used as the internal standard. Infrared spectra were recorded with a PYE/UNICAM Infracord model PU 9516 spectrophotometer in Nujol mulls. Molecular sieves UOP Type 4A (Fluka 69834) and UOP Type 13X (Fluka 69853), reagent grade chemicals, and solvents were used. Compound **11**¹⁵ was prepared according to published procedure.

General Procedure for the Synthesis of Compounds 7a, 7j, 13–15. A solution of 2,4-diamino-6-phenyl[1,3,5]triazine **8** (20 mmol) and the appropriate α-haloketo derivative **9**, **10**, **11**, **12** (30 mmol) in absolute ethanol (100 mL) was stirred under reflux for 30–40 h with small amounts of molecular sieves UOP Type 4A and, when suitable, UOP 13X. After being cooled, the solvent was removed under reduced pressure and the residue was treated with NaHCO₃ saturated aqueous

solution. This alkaline mixture was extracted with ethyl acetate (3 × 20 mL). The combined extracts were dried (Na₂SO₄), reduced to a small volume, and purified by flash chromatography.

7-Methyl-2-phenylimidazo[1,2-*a*][1,3,5]triazin-4-ylamine (7a) and 1-[(7-Methyl-2-phenylimidazo[1,2-*a*][1,3,5]triazin-4-yl)amino]acetone (7j). Eluant: *n*-hexane/ethyl acetate (3:2 v/v). The faster running band gave pure **7j** (36%, mp 290 °C dec), the slower one gave pure **7a** (43%, mp 293 °C dec). Spectroscopic data for **7a**: ¹H NMR (500 MHz, CD₃OD) δ 8.40 (d, *J* = 6.9 Hz, 2H, H-Ar), 7.51–7.41 (m, 3H, H-Ar), 7.35 (s, 1H, H-6), 2.34 (s, 3H, 7-Me); ¹³C NMR (125 MHz, CD₃OD) δ 162.9 (C-2), 152.4, 152.3 (C-4 and C-8a), 143.9 (C-7), 138.1 (C-1'), 131.9, 129.4, 129.2, 104.1 (C-6), 14.1 (Me). Anal. (C₁₂H₁₁N₅) C, H, N. Spectroscopic data for **7j**: ¹H NMR (500 MHz, CDCl₃) δ 8.46 (d, *J* = 7.7 Hz, 2H, H-Ar), 7.51–7.43 (3H, H-Ar), 7.32 (s, 1H, H-6), 4.99 (s, 2H, NCH₂), 2.39 (s, 3H, 7-Me), 2.24 (s, 3H, COMe). IR (Nujol) 1685 cm⁻¹. Anal. (C₁₅H₁₅N₅O) C, H, N.

7-Ethyl-2-phenylimidazo[1,2-*a*][1,3,5]triazin-4-ylamine (13). Eluant: *n*-hexane/ethyl acetate (7:3 v/v). 46%, mp 280 °C dec; ¹H NMR (250 MHz, CD₃OD) δ 8.50 (d, *J* = 8.4 Hz, 2H, H-Ar), 7.62–7.30 (m, 4H, H-Ar and H-6), 2.72 (q, *J* = 7.7 Hz, 2H, CH₂Me), 1.32 (t, *J* = 7.7 Hz, 3H, CH₂Me); ¹³C NMR (125 MHz, CD₃OD) δ 163.1 (C-2), 152.8, 152.6 (C-4 and C-8a), 150.3 (C-7), 138.3 (C-1'), 132.1, 129.5, 129.3, 103.2 (C-6), 23.1 (CH₂), 13.4 (Me). Anal. (C₁₃H₁₃N₅) C, H, N.

7-Isopropyl-2-phenylimidazo[1,2-*a*][1,3,5]triazin-4-ylamine (14). Eluant: *n*-hexane/ethyl acetate (7:3 v/v). 48%, mp 273 °C dec; ¹H NMR (500 MHz, CD₃OD) δ 8.49 (d, *J* = 7.0 Hz, 2H, H-Ar), 7.52–7.49 (m, 3H, H-Ar), 7.66 (s, 1H, H-6), 3.05 (septuplet, *J* = 7.0 Hz, 1H, CH), 1.38 (d, *J* = 7.0 Hz, 6H, 2 × Me); ¹³C NMR (125 MHz, CD₃OD) δ 163.1 (C-2), 152.9, 152.6, 152.3 (C-4 and C-8a and C-7), 138.1 (C-1'), 132.1, 129.5, 129.3, 104.5 (C-6), 75.0 (CH), 27.2 (2 × Me). Anal. (C₁₄H₁₅N₅) C, H, N.

2,7-Diphenylimidazo[1,2-*a*][1,3,5]triazin-4-ylamine (15). Eluant: *n*-hexane/ethyl acetate (4:1 v/v). 38%, mp 356 °C dec; ¹H NMR (500 MHz, CD₃OD) δ 8.51 (d, *J* = 7.3 Hz, 2H, H-Ar), 8.04 (s, 1H, H-6), 7.94 (d, *J* = 8.1 Hz, 2H, H-Ar), 7.55–7.45 (m, 5H, H-Ar), 7.39 (t, *J* = 7.3 Hz, 1H, H-Ar); ¹³C NMR (125 MHz, CD₃OD) δ 162.4 (C-2), 152.3, 152.0 (C-4 and C-8a), 145.7 (C-7), 138.1 (C-1'), 134.2 (C-1''), 132.3, 129.1, 128.3, 128.0, 127.2, 126.1, 103.0 (C-6). Anal. (C₁₇H₁₃N₅) C, H, N.

General Procedure for the Synthesis of Compounds 7b–d. K₂CO₃ (10 mmol) and a catalytic amount of KI were added to a solution of amine **7a** (20 mmol) and the opportune alkyl bromide (30 mmol) in acetonitrile (50 mL). The solution was stirred under reflux for 10–20 h with small amounts of molecular sieves. After being cooled, the solvent was removed under reduced pressure and the residue was treated with NaHCO₃ saturated aqueous solution. This alkaline mixture was extracted with CHCl₃ (3 × 20 mL). The combined extracts were dried (Na₂SO₄), reduced to small volume and purified by flash chromatography.

***N*-Cyclopentyl-*N*-(7-methyl-2-phenylimidazo[1,2-*a*][1,3,5]triazin-4-yl)amine (7b).** Eluant: *n*-hexane/ethyl acetate (3:2 v/v). 41%, mp 298 °C dec; ¹H NMR (500 MHz, DMSO-*d*₆) δ 8.40 (m, 1H, H-Ar), 8.30 (m, 2H, H-Ar), 7.72 (s, 1H, H-6), 7.48 (m, 2H, H-Ar), 4.68 (sextet, *J* = 7.8 Hz, 1H, NCH), 2.28 (s, 3H, 7-Me), 2.15–2.02 (m, 3H, cyclopentyl), 1.82–1.62 (m, 5H, cyclopentyl). Anal. (C₁₇H₁₉N₅) C, H, N.

***N*-(1-Adamantyl)-*N*-(7-methyl-2-phenylimidazo[1,2-*a*][1,3,5]triazin-4-yl)amine (7c).** Eluant: *n*-hexane/ethyl acetate (3:2 v/v). 46%, mp 299 °C dec; ¹H NMR (500 MHz, CDCl₃) δ 8.45 (m, 1H, H-Ar), 8.35 (m, 1H, H-Ar), 7.48–7.46 (m, 3H, H-Ar), 7.27 (s, 1H, H-6), 2.58 (m, 2H, adamantyl), 2.50 (m, 1H, adamantyl), 2.47 (m, 1H, adamantyl), 2.45 (m, 1H, adamantyl), 2.26 (s, 3H, Me), 2.19–2.17 (m, 4H, adamantyl), 1.76 (m, 6H, adamantyl). Anal. (C₂₂H₂₅N₅) C, H, N.

***N*-(Cyclohexylmethyl)-*N*-(7-methyl-2-phenylimidazo[1,2-*a*][1,3,5]triazin-4-yl)amine (7d).** Eluant: *n*-hexane/ethyl acetate (3:2 v/v). 45%, mp 220 °C dec; ¹H NMR (500 MHz, CD₃OD) δ 8.45 (d, *J* = 6.5 Hz, 2H, H-Ar), 7.50–7.47 (m, 3H,

H-Ar), 7.43 (s, 1H, H-6), 3.60 (d, $J = 6.6$ Hz, 2H, NCH₂), 2.38 (s, 3H, 7-Me), 1.90–1.77 (m, 4H, cyclohexyl), 1.75–1.63 (m, 1H, cyclohexyl), 1.34–1.25 (m, 4H, cyclohexyl), 1.13–1.05 (m, 2H, cyclohexyl). Anal. (C₁₉H₂₃N₅) C, H, N.

N-(Benzyl)-N-(7-methyl-2-phenylimidazo[1,2-*a*][1,3,5]triazin-4-yl)amine (7e). K₂CO₃ (10 mmol) and a catalytic amount of KI were added to a solution of **7a** (20 mmol) and benzyl bromide (30 mmol) in acetonitrile (50 mL). The solution was stirred under reflux for 10 h. After being cooled, the solvent was removed under reduced pressure and the residue was treated with concentrated NH₄OH and warmed to reflux for 10 h. This alkaline mixture was then extracted with CHCl₃ (3 × 20 mL). The combined extracts were dried (Na₂SO₄), reduced to a small volume and purified by flash chromatography (eluant: *n*-hexane/ethyl acetate 3:2 v/v). 48%, mp 186 °C dec; ¹H NMR (500 MHz, CDCl₃) δ 8.57 (d, $J = 7.6$ Hz, 2H, H-Ar), 7.52–7.43 (m, 3H, H-Ar), 7.40–7.32 (m, 2H, H-Ar), 7.31–7.27 (m, 4H, H-Ar and H-6), 5.39 (s, 2H, NCH₂), 2.27 (s, 3H, 7-Me). Anal. (C₁₉H₁₇N₅) C, H, N.

General Procedure for the Synthesis of N-(7-Methyl-2-phenylimidazo[1,2-*a*][1,3,5]triazin-4-yl)acetamide (7f) and N-(2,7-Diphenylimidazo[1,2-*a*][1,3,5]triazin-4-yl)acetamide (7r). Acetic anhydride (15 mmol) was added to a solution of **7a** or **15** (10 mmol) and 4-(dimethylamino)pyridine (5 mmol) in anhydrous THF (20 mL). The solution was kept at 0 °C for 1 h and was then added with NaHCO₃ saturated aqueous solution (40 mL) and extracted with CHCl₃ (3 × 20 mL). The combined extracts were dried (Na₂SO₄), the solvent was evaporated and the residue was treated with diethyl ether to obtain a precipitate collected by filtration and identified as pure **7f** or **7r**.

N-(7-Methyl-2-phenylimidazo[1,2-*a*][1,3,5]triazin-4-yl)acetamide (7f). 70%, mp 261 °C dec; ¹H NMR (500 MHz, CDCl₃) δ 8.30 (m, 2H, H-Ar), 7.56–7.51 (m, 3H, H-Ar), 7.50 (s, 1H, H-6), 2.51 (s, 3H, 7-Me), 2.22 (s, 3H, COMe). Anal. (C₁₄H₁₃N₅O) C, H, N.

N-(2,7-Diphenylimidazo[1,2-*a*][1,3,5]triazin-4-yl)acetamide (7r). 20%, mp 353 °C dec; ¹H NMR (500 MHz, DMSO-*d*₆) δ 8.54 (s, 1H, H-6), 8.42 (m, 2H, H-Ar), 7.97 (d, $J = 7.4$ Hz, 2H, H-Ar), 7.60–7.55 (m, 3H, H-Ar), 7.52 (t, $J = 7.4$ Hz, 2H, H-Ar), 7.40 (t, $J = 7.4$ Hz, 1H, H-Ar), 2.58 (s, 3H, COMe). Anal. (C₁₉H₁₅N₅O) C, H, N.

General Procedure for the Synthesis of Compounds 7g-i,k-q. K₂CO₃ (10 mmol) and a catalytic amount of KI were added to a solution of amine **7a** (or **13**, **14**, **15**) (20 mmol) and the opportune alkyl or acyl chloride (30 mmol) in acetonitrile (50 mL). The solution was stirred under reflux for 10–20 h with small amounts of molecular sieves. After being cooled, the solvent was removed under reduced pressure and the residue was treated with NaHCO₃ saturated aqueous solution. This alkaline mixture was extracted with CHCl₃ (3 × 20 mL). The combined extracts were dried (Na₂SO₄), reduced to small volume, and purified by flash chromatography.

N-(7-Methyl-2-phenylimidazo[1,2-*a*][1,3,5]triazin-4-yl)cyclopentanecarboxamide (7g). Eluant: *n*-hexane/ethyl acetate (7:3 v/v). 62%, mp 245 °C dec; ¹H NMR (500 MHz, CDCl₃) δ 8.16 (d, $J = 5.7$ Hz, 2H, H-Ar), 7.61–7.50 (m, 4H, H-Ar and H-6), 3.21 (m, 1H, COCH), 2.45 (s, 3H, 7-Me), 2.08–1.89 (m, 4H, cyclopentyl), 1.80–1.78 (m, 2H, cyclopentyl), 1.68–1.63 (m, 2H, cyclopentyl). Anal. (C₁₈H₁₉N₅O) C, H, N.

N-(7-Methyl-2-phenylimidazo[1,2-*a*][1,3,5]triazin-4-yl)cyclohexanecarboxamide (7h). Eluant: *n*-hexane/ethyl acetate (7:3 v/v). 54%, mp 254 °C dec; ¹H NMR (500 MHz, CDCl₃) δ 8.22 (m, 2H, H-Ar), 7.58–7.53 (m, 3H, H-Ar), 7.45 (s, 1H, H-6), 2.45 (s, 3H, Me), 2.05 (d, $J = 12.5$ Hz, 2H, cyclohexyl), 1.84 (d, $J = 12.8$ Hz, 2H, cyclohexyl), 1.73 (d, $J = 13.2$ Hz, 1H, cyclohexyl), 1.40–1.37 (m, 4H, cyclohexyl), 1.29–1.24 (m, 2H, cyclohexyl). Anal. (C₁₉H₂₁N₅O) C, H, N.

N-(7-Methyl-2-phenylimidazo[1,2-*a*][1,3,5]triazin-4-yl)benzencarboxamide (7i). Eluant: *n*-hexane/ethyl acetate (7:3 v/v). 42%, mp 284 °C dec; ¹H NMR (500 MHz, CDCl₃) δ 8.57 (d, $J = 8.1$ Hz, 2H, H-Ar), 8.21 (d, $J = 7.3$ Hz, 2H, H-Ar), 7.66–7.57 (m, 5H, H-Ar and H-6), 7.50 (t, $J = 8.1$ Hz, 2H, H-Ar), 2.50 (s, 3H, 7-Me). Anal. (C₁₉H₁₅N₅O) C, H, N.

1-[(7-Methyl-2-phenylimidazo[1,2-*a*][1,3,5]triazin-4-yl)amino]butanone (7k). Eluant: *n*-hexane/ethyl acetate (7:3 v/v). 34%, mp 182 °C dec; ¹H NMR (500 MHz, CDCl₃) δ 8.50 (d, $J = 8.4$ Hz, 2H, H-Ar), 7.56–7.45 (m, 3H, H-Ar), 7.35 (s, 1H, H-6), 5.06 (s, 2H, NCH₂), 2.68 (q, $J = 7.9$ Hz, 2H, CH₂Me), 2.28 (s, 3H, 7-Me), 1.20 (t, $J = 7.9$ Hz, 3H, CH₂Me). IR (Nujol) 1690 cm⁻¹. Anal. (C₁₆H₁₇N₅O) C, H, N.

N-(7-Ethyl-2-phenylimidazo[1,2-*a*][1,3,5]triazin-4-yl)cyclopentanecarboxamide (7l). Eluant: *n*-hexane/ethyl acetate (7:3 v/v). 50%, mp 239 °C dec; ¹H NMR (500 MHz, CDCl₃) δ 8.18 (m, 2H, H-Ar), 7.57–7.50 (m, 4H, H-Ar and H-6), 3.08–2.92 (m, 1H, COCH), 2.82 (q, $J = 7.8$ Hz, 2H, CH₂Me), 2.12–1.79 (m, 4H, cyclopentyl), 1.70–1.59 (m, 4H, cyclopentyl), 1.37 (t, $J = 7.8$ Hz, 3H, CH₂Me). Anal. (C₁₉H₂₁N₅O) C, H, N.

N-(7-Isopropyl-2-phenylimidazo[1,2-*a*][1,3,5]triazin-4-yl)cyclopentanecarboxamide (7m). Eluant: *n*-hexane/ethyl acetate (7:3 v/v). 53%, mp 234 °C dec; ¹H NMR (500 MHz, CDCl₃) δ 8.24 (d, $J = 7.0$ Hz, 2H, H-Ar), 7.75–7.49 (m, 4H, H-Ar and H-6), 3.12 (quintet, $J = 8.1$ Hz, 1H, COCH), 2.18 (d, $J = 7.1$ Hz, 6H, 2xMe), 2.15–1.93 (m, 5H, cyclopentyl and CH), 1.86–1.67 (m, 4H, cyclopentyl). Anal. (C₂₀H₂₃N₅O) C, H, N.

N-(2,7-Diphenylimidazo[1,2-*a*][1,3,5]triazin-4-yl)cyclopentanecarboxamide (7n). Eluant: *n*-hexane/ethyl acetate (7:3 v/v). 45%, mp 220 °C dec; ¹H NMR (500 MHz, CDCl₃) δ 8.23 (d, $J = 7.3$ Hz, 2H, H-Ar), 8.07–8.04 (m, 3H, H-Ar), 7.68–7.36 (m, 6H, H-Ar and H-6), 3.10 (quintet, $J = 7.7$ Hz, 1H, COCH), 2.10–1.90 (m, 4H, cyclopentyl), 1.83–1.61 (m, 4H, cyclopentyl). Anal. (C₂₃H₂₁N₅O) C, H, N.

1-[(7-Ethyl-2-phenylimidazo[1,2-*a*][1,3,5]triazin-4-yl)amino]acetone (7o). Eluant: *n*-hexane/ethyl acetate (7:3 v/v). 25%, mp 276 °C dec; ¹H NMR (500 MHz, CDCl₃) δ 8.41 (d, $J = 7.6$ Hz, 2H, H-Ar), 7.48–7.39 (m, 3H, H-Ar), 7.22 (s, 1H, H-6), 4.93 (s, 2H, NCH₂), 2.46 (q, $J = 7.5$ Hz, 2H, CH₂Me), 2.34 (s, 3H, COMe), 1.30 (t, $J = 7.5$ Hz, 3H, CH₂Me). IR (Nujol) 1685 cm⁻¹. Anal. (C₁₆H₁₇N₅O) C, H, N.

1-[(7-Isopropyl-2-phenylimidazo[1,2-*a*][1,3,5]triazin-4-yl)amino]acetone (7p). Eluant: *n*-hexane/ethyl acetate (7:3 v/v). 24%, mp 269 °C dec; ¹H NMR (500 MHz, CDCl₃) δ 8.46 (d, $J = 7.7$ Hz, 2H, H-Ar), 7.46 (m, 1H, H-Ar), 7.45 (m, 2H, H-Ar), 7.35 (s, 1H, H-6), 5.00 (s, 2H, NCH₂), 2.75 (septuplet, $J = 6.9$ Hz, 1H, CH), 2.39 (s, 3H, COMe), 1.33 (d, $J = 6.9$ Hz, 6H, 2xMe). IR (Nujol) 1686 cm⁻¹. Anal. (C₁₇H₁₉N₅O) C, H, N.

1-[(2,7-Diphenylimidazo[1,2-*a*][1,3,5]triazin-4-yl)amino]acetone (7q). Eluant: *n*-hexane/ethyl acetate (7:3 v/v). 20%, mp 353 °C dec; ¹H NMR (500 MHz, CDCl₃) δ 8.49 (d, $J = 7.4$ Hz, 2H, H-Ar), 7.57 (s, 1H, H-6), 7.55–7.52 (m, 4H, H-Ar), 7.50–7.48 (m, 2H, H-Ar), 7.43–7.37 (m, 2H, H-Ar), 4.97 (s, 2H, NCH₂), 2.29 (s, 3H, COMe). IR (Nujol) 1687 cm⁻¹. Anal. (C₂₀H₁₇N₅O) C, H, N.

Receptor Binding Assays. A₁, A_{2A}, and A₃ Receptor Binding. Displacement of [³H]CHA (31Ci/mmol) from A₁AR in bovine cortical membranes, [³H]CGS21680 (42.1Ci/mmol) from A_{2A}AR in bovine striatal membranes and [¹²⁵I]AB-MECA (2000Ci/mmol) from A₃AR in bovine cortical membranes were performed as described elsewhere.⁸

Compounds were dissolved in DMSO and added to the assay mixture (DMSO concentration maximum 2%). Blank experiments were carried out to determine the effect of solvent on binding. Protein estimation was based on a reported method,¹⁶ after solubilization with 0.75N sodium hydroxide, using bovine serum albumin as standard. At least six different concentrations of each compound were used. The experiments ($n = 4$), carried out in triplicate, were analyzed by an iterative curve-fitting procedure (GraphPad, Prism program, San Diego, CA), which provided IC₅₀, K_i , and SEM values for tested compounds.

The dissociation constant (K_d) of [³H]CHA, [³H]CGS21680 and [¹²⁵I]AB-MECA was 1.2, 14, and 1.02 nM, respectively.

Computational Chemistry. All molecular modeling was performed using the software package SYBYL¹⁷ running on a Silicon Graphics R10000 workstation. Molecular models of imidazotriazine derivatives were built according to SYBYL

standard bond lengths and valence angles. Geometry optimizations were realized with the SYBYL/MAXIMIN2 minimizer by applying the BFGS algorithm¹⁸ and setting a root-mean-square gradient of the forces acting on each atom at 0.05 kcal/mol Å as a convergence criterion. Molecular graphics, root-mean-squares (rms) fit, and calculations of ring centroids of substructures were also carried out using SYBYL.

Docking simulations were carried out starting from the previously published bovine A₁AR model,⁸ which was built using as template the frog rhodopsin,^{19,20} a membrane protein belonging to the G-protein coupled receptors (GPCRs) superfamily. Additional details regarding the receptor structure, site-directed mutagenesis data and methods applied in developing the A₁AR model are reported in ref 8. The model has also been compared with the rhodopsin template recently published by Palczewski and co-workers.²¹ Although slight differences in the orientation of the helices in the transmembrane domain are apparent; the juxtaposition of the residues within the putative adenosine binding pocket is well-conserved between the two models.

The position of the docked ligand **5** (Chart 1) in the receptor model⁸ was taken as a starting point. Selected ITAs (**7g** and **7j**) were docked into the receptor model by means of the following steps: (i) superposition on the docked compound **5** about the NH atoms plus the centroid of the pendant phenyl ring; (ii) removal of **5** from the receptor; (iii) energy-minimization of the resulting ligand/binding site complexes based on the molecular mechanics Tripos force field.²²

Molecular dynamics simulations of the **7j**/A₁AR complex were performed with the SYBYL/DYNAMICS module under default settings. These simulations, in which the protein backbone was treated as a rigid aggregate, were run at 300 K for 50 ps after reaching equilibration. Five structures extracted at 10, 20, 30, 40, and 50 ps were selected and energy-minimized. Figure 3, displaying the interaction between **7j** and the side chains of residues within a distance of 5 Å from any atom of the bound ligand, refers to the last MD snapshot.

References

- Ravelich, V.; Burnstock, G. Receptors for Purines and Pyrimidines. *Pharmacol. Rev.* **1998**, *50*, 413–492.
- Olah, M.; Stiles, G. L. The Role of Receptor Structure in Determining Adenosine Receptor Activity. *Pharmacol. Ther.* **2000**, *85*, 55–75.
- Impagnatiello, F.; Bastia, E.; Ongini, E.; Monopoli, A. Adenosine Receptors in Neurological Disorders. *Emerging Ther. Targets* **2000**, *4*, 635–663.
- Müller, C. E. Adenosine Receptor Ligands – Recent Developments. Part I. Agonists. *Curr. Med. Chem.* **2000**, *7*, 1269–1288.
- Müller, C. E. A1-Adenosine Receptor Antagonists. *Exp. Opin. Ther. Pat.* **1997**, *7*, 419–440.
- Poulsen, S. A.; Quinn, R. J. Adenosine Receptors for Future Drugs. *Bioorg. Med. Chem.* **1998**, *6*, 619–641.
- Hess, S. Recent Advances in Adenosine Receptor Antagonist Research. *Exp. Opin. Ther. Pat.* **2001**, *11*, 1533–1561.
- Da Settimo, F.; Primofiore, G.; Taliani, S.; Marini, A. M.; La Motta, C.; Novellino, E.; Greco, G.; Lavecchia, A.; Trincavelli, L.; Martini, C. 3-Aryl[1, 2, 4]triazolo[4, 3-*a*]benzimidazol-4(10*H*)-ones: A New Class of Selective A₁ Adenosine Receptor Antagonists. *J. Med. Chem.* **2001**, *44*, 316–327.
- Hamilton, H. W.; Ortwine, D. F.; Worth, D. F.; Bristol, J. A. Synthesis and Structure–Activity Relationships of Pyrazolo[4,3-*d*]pyrimidin-7-ones as Adenosine Receptor Antagonists. *J. Med. Chem.* **1987**, *30*, 91–96.
- Sarges, R.; Howard, H. R.; Browne, R. G.; Lebel, L. A.; Seymour, P. A.; Koe, B. K. 4-Amino[1,2,4]triazolo[4, 3-*a*]quinoxalines. A Novel Class of Potent Triazoloquinazoline Adenosine Receptor Antagonists and Potential Rapid-Onset Antidepressants. *J. Med. Chem.* **1990**, *33*, 2240–2254.
- Francis, J. E.; Cash, W. D.; Psychoyos, S.; Ghai, G.; Wenk, P.; Friedmann, R. C.; Atkins, C.; Warren, V.; Furness, P.; Hyun, J. L.; Stone, G. A.; Desai, M.; Williams, M. Structure–Activity Profile of a Series of Novel Triazoloquinazoline Adenosine Antagonists. *J. Med. Chem.* **1988**, *31*, 1014–1020.
- van Galen, P. J. M.; Nissen, P.; Van Wijngaarden, I.; IJzerman, A. P.; Soudijn, W. 1*H*-Imidazo[4, 5-*c*]quinolin-4-amine: Novel Non-Xanthine Adenosine Antagonists. *J. Med. Chem.* **1991**, *34*, 1202–1206.
- Suzuki, F.; Shimada, J.; Nonaka, H.; Ishii, A.; Shiozaki, S.; Ichikawa, S.; Ono, E. 7,8-Dihydro-8-ethyl-2-(3-noradamantyl)-4-propyl-1*H*-imidazo[2,1-*b*]purin-5(4*H*)-one: A Potent and Water-Soluble Adenosine A₁ Antagonist. *J. Med. Chem.* **1992**, *35*, 3578–3581.
- Sacchi, A.; Laneri, S.; Arena, F.; Luraschi, E.; Abignente, E.; D'Amico, M.; Berrino, L.; Rossi, F. Research on Heterocyclic Compounds. Part XXXVI. Imidazo[1,2-*a*]pyrimidine-2-acetic Derivatives: Synthesis and Antiinflammatory Activity. *Eur. J. Med. Chem.* **1997**, *32*, 677–682.
- Gaudry, M.; Marquet, A. 1-Bromo-3-methyl-2-butanone. *Org. Synth.* **1976**, *55*, 24–27.
- Lowry, O. H.; Rosebrough, N. J.; Farr, A. L.; Randall, R. J. Protein Measurement With the Folin Phenol Reagent. *J. Biol. Chem.* **1951**, *193*, 265–275.
- Sybyl Molecular Modelling System (version 6.2), Tripos Inc., St. Louis, MO.
- Head, J.; Zerner, M. C. A Broyden-Fletcher-Goldfarb-Shanno Optimization Procedure for Molecular Geometries. *Chem. Phys. Lett.* **1985**, *122*, 264–274.
- Unger, V. M.; Hargrave, P. A.; Baldwin, J. M.; Schertler, G. F. X. Arrangement of Rhodopsin Transmembrane Alpha Helices Obtained by Electron Cryo-microscopy. *Nature* **1997**, *389*, 203–206.
- Baldwin, J. M.; Schertler, G. F. X.; Unger, V. M. An Alpha-carbon Template for the Transmembrane Helices in the Rhodopsin Family of G-protein-coupled Receptors. *J. Mol. Biol.* **1997**, *272*, 144–164.
- Palczewski, K.; Kumasaka, T.; Hori, T.; Behnke, C. A.; Motoshima, H.; Fox, B. A.; Le Trong, I.; Teller, D. C.; Okada, T.; Stenkamp, R. E.; Yamamoto, M.; Miyano, M. Crystal Structure of Rhodopsin: A G Protein-Coupled Receptor. *Science* **2000**, *289*, 739–745.
- Vinter, J. G.; Davis, A.; Saunders, M. R. Strategic Approaches to Drug Design. 1. An Integrated Software Framework for Molecular Modelling. *J. Comput.-Aided Mol. Design* **1987**, *1*, 31–55.

JM020911E